Available online at http://www.journalcra.com

International Journal of Current Research
Vol. 7, Issue, 05, pp.16433-16439, May, 2015

INTERNATIONAL JOURNAL OF CURRENT RESEARCH

ISSN: 0975-833X

RESEARCH ARTICLE

NEW HEXA BISMUTH- TIN BASED ALLOYS FOR ELECTRICAL FUSE AND NUCLEAR APPLICATIONS

[1]Abu Bakr El- Bediwi, [2,*]Feryal Dawood, [3]Mustafa Kamal

[1,3]Metal Physics Lab., Physics Department, Faculty of Science, Mansoura University, Mansoura, Egypt
[2]Basic Education College, University of Diayala, Iraq

ARTICLE INFO

Article History:
Received 07th February, 2015
Received in revised form
23rd March, 2015
Accepted 28th April, 2015
Published online 31st May, 2015

Key words:
Electrical Fuse Alloy,
Thermal Parameters,
Structure,
Elastic Modulus,
Internal Friction,
Hardness,
TiO_2, Electrical Resistivity

ABSTRACT

Structural, electrical resistivity, thermal and mechanical properties of Bi- Sn- Pb- Cd- In- TiO_2 and Bi- Sn- Pb- Zn- In- Ag alloys have been investigated. Melting temperature of Bi- Sn- Pb- Cd- In- TiO_2 alloys increased with increasing TiO_2 content and decreasing Bi content. Elastic modulus, Vickers hardness, internal friction, electrical resistivity and thermal parameters varied with increasing TiO_2 content and decreasing Bi content. Melting temperature, internal friction, Vickers hardness of Bi- Sn- Pb- Zn- In- Ag alloys decreased with increasing Bi content and decreasing Sn content. Elastic modulus and electrical resistivity of Bi- Sn- Pb- Zn- In- Ag alloys increased with increasing Bi content and decreasing Sn content. The $Bi_{49}Pb_{15}Sn_{22}Cd_3In_{10}(TiO_2)_1$ alloy has best properties (low melting point= 91 ºC, high elastic modulus= 36.2 GPa, high Vickers hardness= 19.1 kg\mm^2, and lower internal friction= 0.055) for nuclear applications. The $Bi_{25}Sn_{62.5}Pb_3Zn_3In_4Ag_{2.5}$ alloy has best properties (low coast, low melting point= 174 ºC, high elastic modulus= 30.6 GPa, high Vickers hardness= 19.25 kg\mm^2, and adequate internal friction= 0.078) for electrical fuse.

Citation Abu Bakr El- Bediwi, Feryal Dawood, Mustafa Kamal, 2015. "New hexa bismuth- tin based alloys for electrical fuse and nuclear applications", *International Journal of Current Research*, 7, (5), 16433-16439.

INTRODUCTION

Electrical fuse is a device used to protect load or source from overcurrent. It is a simple, less resistive, self-sacrificial and cheapest device used to interrupt a circuit under short circuit, excessive overload or over current conditions. Low temperature alloys, which typically contain indium or bismuth, melt at temperatures less than 180 °C. These low-melting alloys are required for a wide variety of applications. The material used as fuse element must have low melting point, low ohmic resistance, high conductivity and low cost. There is no such material that satisfies all these properties. The materials commonly used for fuse elements are tin, lead, silver, copper, zinc, aluminum and alloys of lead and tin. The wide spread usage of lead-tin-bismuth fusible alloy solders is due primarily to the combination of low cost commercial microelectronics and convenient material property (McCormack *et al*., 1996). They are used in soldering operations where they should remain approximately below 183 °C. These alloys contain bismuth as about 50 percent.

Corresponding author: Feryal Dawood,
Basic education college, University of Diayala, Iraq.

Fusible alloys are also widely used in radio-therapy procedures to shield organs at risk or to shape the radiation field (Davis and Reiner, 1995; Marrs *et al*., 1993) since originally suggested in 1973 by Powers *et al*. (1973). Also cadmium free fusible lead alloy suitable for custom radiotherapy shielding blocks (Blackwell and Amundson, 1990). Because bismuth alloys have better properties, such as very low melting temperatures and low physical strength, for their extensive uses (different applications) many researches were done to evaluate and discuss structure and physical properties of quenched bismuth-tin eutectic alloy, bismuth- lead eutectic alloy, bismuth- lead-tin, bismuth- lead- tin- cadmium, tin- antimony and the effect of adding alloying elements to these alloys (Glazer, 1994; Kamal *et al*., 2006; El-Bediwi and El-Bahay, 2004; Kamal and El-Bediwi, 2004; El-Bediwi *et al*., 2004; El-Bediwi *et al*., 2004; Kamal *et al*., 1997; Kamal *et al*., 1998; Kamal and El-Bediwi, 2002; El-Bediwi, 2002; Kamal *et al*., 2004; Kamal *et al*., 2004; Kamal *et al*., 2005). The aim of the present work is to produce new hexa fusible alloys (by adding different elements such as Cd, Zn, In and TiO_2 to Bi- Sn matrix) with superior properties for fuse electronic and nuclear applications.

Experimental work

Bi- Sn- Pb- Cd- In- TiO_2 and Bi- Sn- Pb- Zn- In- Ag alloys were made from high purity bismuth (99.99%), tin (99.99%), lead (99.95%), zinc (99.95%), cadmium (99.95%), indium (99.99%), silver (99.99%) and TiO_2(99%) by conventional melting techniques. The resulting ingots were turned and re-melted four times to increase the homogeneity. From these ingots, long ribbons of about 4 mm width and ~70 µm thickness were prepared by a single roller method in air (melt spinning technique). The surface velocity of the roller was 31.4 m/s giving a cooling rate of ~3.7 × 10^5 K/s. The samples then cut into convenient shape for the measurements using double knife cuter. X–ray diffraction analysis was performed on the flat surface of all samples using an X–ray Diffractometer (Dx–30, Shimadzu, Japan) of Cu–Kα radiation with λ=1.54056 Å at 45 kV and 35 mA and Ni–filter in the angular range 2θ ranging from 20 to 100° in continuous mode with a scan speed 5 deg/min. Phase identification was carried out by matching each characteristic peak with the Data Cards.

Scanning electron microscope JEOL JSM-6510LV, Japan was used to study microstructure of used samples. The melting endotherms of used alloys were obtained using a SDT Q600 V20.9 Build 20 instrument. The Double Bridge method was used to measure the electrical resistivity for the used alloys, which has been shown to be sensitive in the range 10^{-6} to 1.0 Ω.A digital Vickers micro-hardness tester, (Model-FM-7-Japan), was used to measure Vickers hardness values of used alloys. Internal friction Q^{-1} and the elastic constants of used alloys were determined using the dynamic resonance method (Schreiber *et al*., 1973; Timoshenko and Goddier, 1951; Nuttall, 1971).

RESULTS AND DISCUSSIONS

Microstructure

X-ray diffraction patterns of $Bi_{50-x}Pb_{15}Sn_{22}Cd_3In_{10}(TiO_2)_x$(x= 0.5, 1, 1.5) alloys have lines corresponding to rhombohedral Bi phase, tetragonal Sn phase, face centered cubic Pb phase, hexagonal Cd phase, face centered cubic In phase, Pb_7Bi_3 and

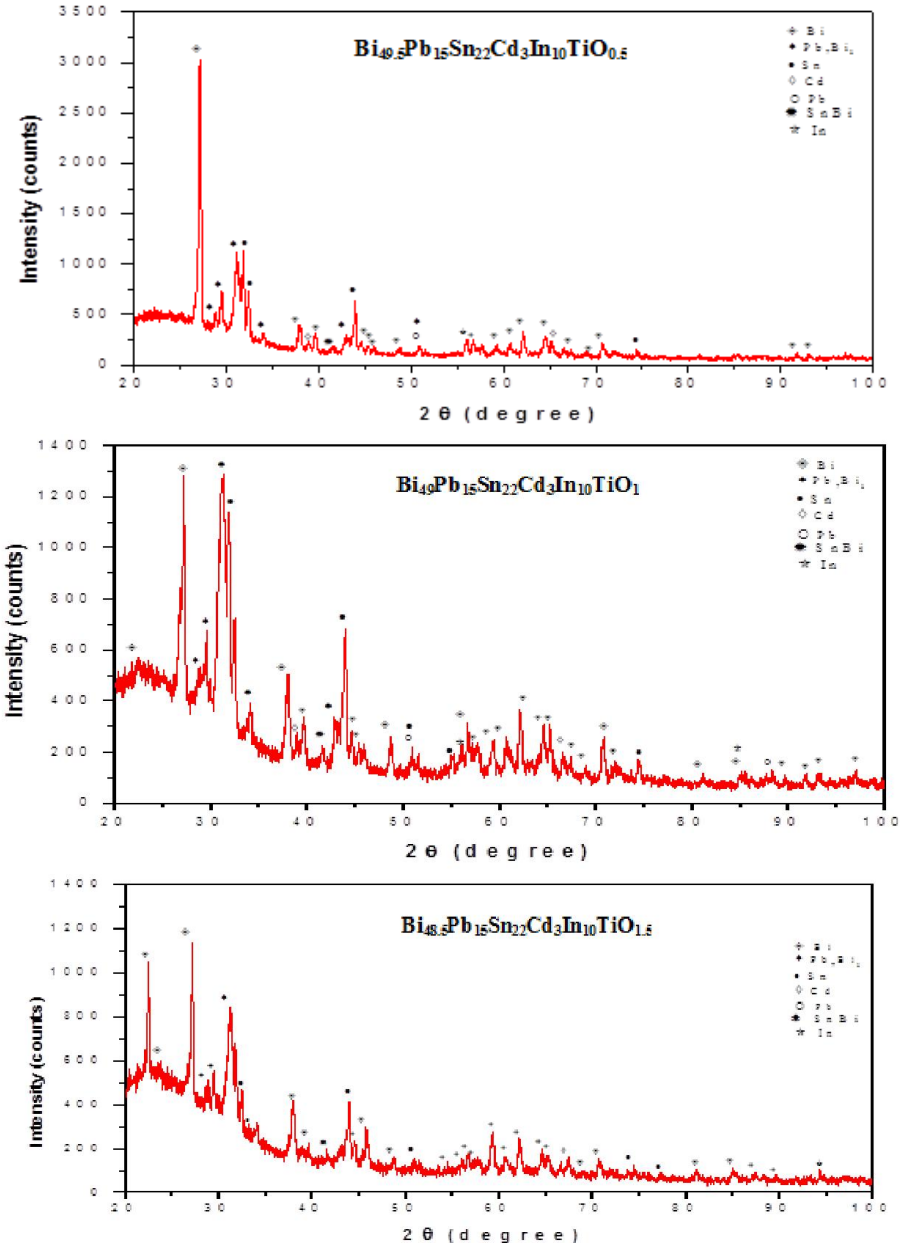

Figure 1a. x-ray diffraction patterns of $Bi_{50-x}Pb_{15}Sn_{22}Cd_3In_{10}(TiO_2)_x$ alloys

SnBi intermetallic compounds as shown in Figure 1a. X-ray analysis of $Bi_{50-x}Pb_{15}Sn_{22}Cd_3In_{10}(TiO_2)_x$ alloys also show that, a change in featureformed phases (peak intensity, peak broadness, miller indices, position (2θ), and area under peaks) which dependent on (TiO_2) ratio in the alloy. Lattice parameters, (a and c), and unit volume cell (V) of rhombohedral Bi phase in $Bi_{50-x}Pb_{15}Sn_{22}Cd_3In_{10}(TiO_2)_x$ alloys were determined and then listed in Table 1a.

Table 1a:-lattice parameters, unit cell volume and crystal size of Bi in $Bi_{50-x}Pb_{15}Sn_{22}Cd_3In_{10}(TiO_2)_x$ alloys

Alloys	a_{rho} Å	c Å	V Å^3	τ Å
$Bi_{49.5}Pb_{15}Sn_{22}Cd_3In_{10}(TiO_2)_{0.5}$	4.676	11.61	69.296	283.29
$Bi_{49}Pb_{15}Sn_{22}Cd_3In_{10}(TiO_2)_1$	4.681	11.625	69.437	356.94
$Bi_{48.5}Pb_{15}Sn_{22}Cd_3In_{10}(TiO_2)_{1.5}$	4.789	12.01	71.774	301.45

The results show that, a little variation caused in Bi lattice parameters and unit cell volume but crystal particle size of it has a significant change with increasing (TiO_2) and decreasing Bi content. X-ray diffraction patterns of $Bi_{45.5}Sn_{42}Pb_3Zn_3In_4Ag_{2.5}$ alloy has lines corresponding to rhombohedral Bi phase, tetragonal Sn phase, face centered cubic Pb phase, Zn phase, Pb_7Bi_3 and SnBi intermetallic compounds as shown in Figure 1b. But $Bi_{25}Sn_{62.5}Pb_3Zn_3In_4Ag_{2.5}$ alloy has lines corresponding to rhombohedral Bi phase and tetragonal Sn phase as shown in Figure 1b.X-ray analysis of $Bi_{45.5}Sn_{42}Pb_3Zn_3In_4Ag_{2.5}$ and $Bi_{25}Sn_{62.5}Pb_3Zn_3In_4Ag_{2.5}$ alloys also show that, a change in formed phases shape (peak intensity, broadness of peak, miller indices, position (2θ), and area under peaks) which dependent on the alloy composition.

Also lattice parameters, (a and c), unit volume cell (V) and crystal size of rhombohedral Bi phase and tetragonal Sn phase in Bi-Sn- Pb- In- Zn- Ag alloys were determined and then listed in Table 1b. Scanning electron micrographs, SEM, of $Bi_{50-x}Pb_{15}Sn_{22}In_{10}Cd_3(TiO_2)_x$ (x=0 or 1.5 wt.%) and $Bi_{25}Sn_{62.5}Pb_3Zn_3In_4Ag_{2.5}$ alloys show heterogeneous structure as shown in Figure 2 which agreed with x-ray analysis. Also it clears that, microstructure of these alloys dependent on the alloy composition.

Thermal properties

The DTA-curve is primarily used for detecting and characterizing thermal processes (such as endothermic/exothermic) qualitatively. DTA can therefore be used to study thermal properties and phase changes which do not lead to a change in enthalpy. The baseline of the DTA curve should then exhibit discontinuities at the transition temperatures and the slope of the curve at any point will depend on the microstructural constitution at that temperature. Thermal analysis is used to study solid state transformations as well as solid-liquid reactions. Figure 3a shows DSC thermographs of $Bi_{50-x}Pb_{15}Sn_{22}Cd_3In_{10}(TiO_2)_x$ (x= 0.5, 1, 1.5). Also Figure 3b shows DSC thermographs of $Bi_{45.5}Sn_{42}Pb_3Zn_3In_4Ag_{2.5}$ and $Bi_{25}Sn_{62.5}Pb_3Zn_3In_4Ag_{2.5}$ alloys. DSC thermographs show a variation occurred in exo-thermic peaks of used alloys and it's dependent on alloys composition. The melting temperature and other thermal properties of $Bi_{50-x}Pb_{15}Sn_{22}Cd_3In_{10}(TiO_2)_x$, $Bi_{45.5}Sn_{42}Pb_3Zn_3In_4Ag_{2.5}$ and $Bi_{25}Sn_{62.5}Pb_3Zn_3In_4Ag_{2.5}$ alloys are listed in Table 2.

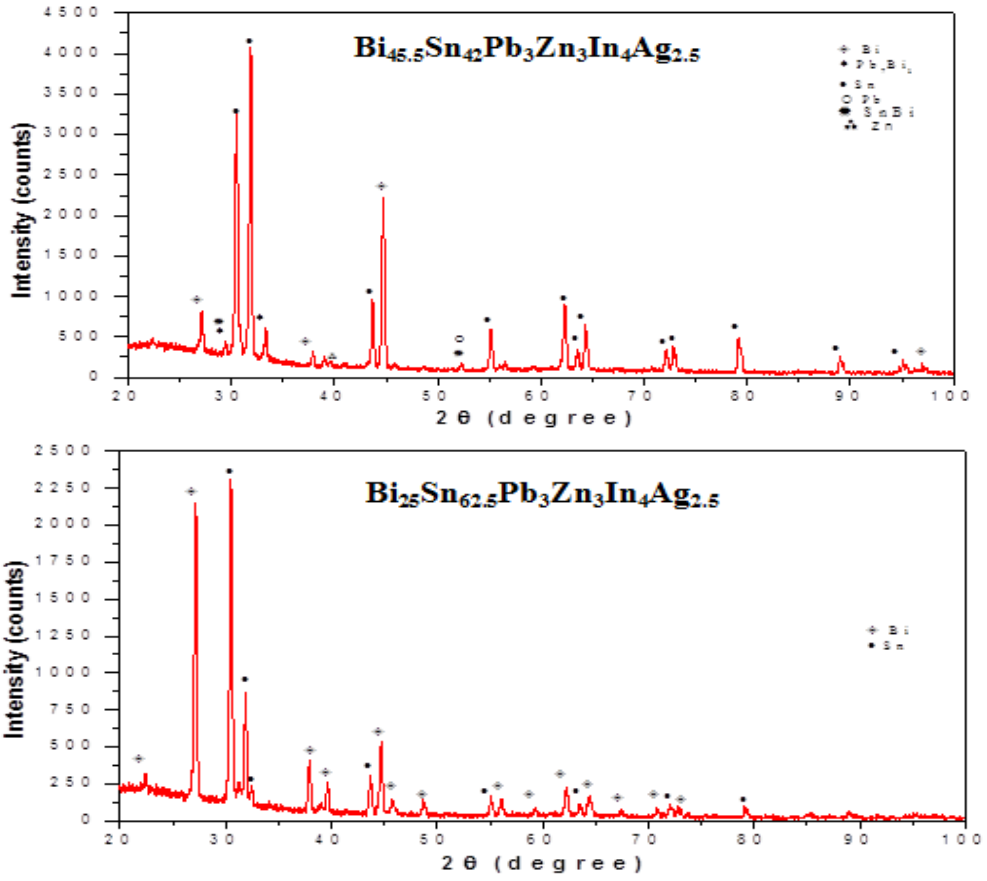

Figure 1b.- x-ray diffraction patterns of Bi-Sn-Pb-Zn-In-Ag alloys

Table 1b. Lattice parameters, unit cell volume and crystal size of Bi and Sn in Bi-Sn-Pb-Zn-In-Ag alloys

Alloys	a_{rho}Å	c Å	V Å^3	τ Å
$Bi_{45.5}Sn_{42}$	4.753	11.886	70.75	(Bi) 334.75
$Pb_3Zn_3In_4Ag_{2.5}$	5.864	3.191	109.727	(Sn) 343.52
$Bi_{25}Sn_{62.5}$	4.776	11.97	70.829	(Bi)
$Pb_3Zn_3In_4Ag_{2.5}$	5.855	3.199	109.649	301.74 (Sn) 424.89

$Bi_{50}Pb_{15}Sn_{22}Cd_3In_{10}$

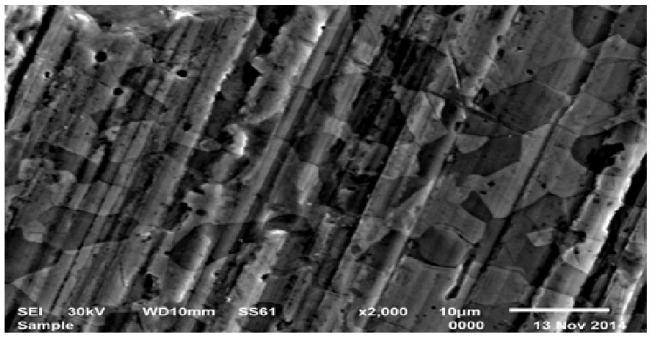

$Bi_{48.5}Pb_{15}Sn_{22}Cd_3In_{10}(TiO_2)_{1.5}$

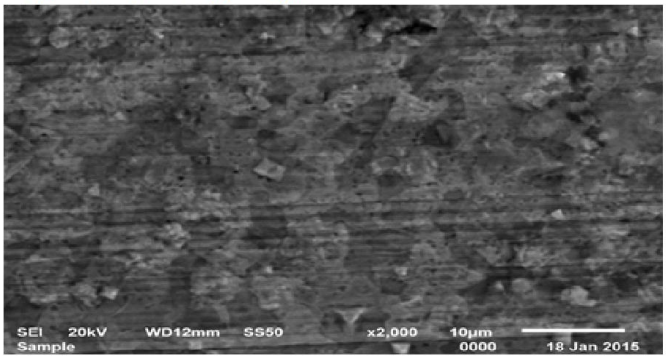

$Bi_{25}Sn_{62.5}Pb_3Zn_3In_4Ag_{2.5}$

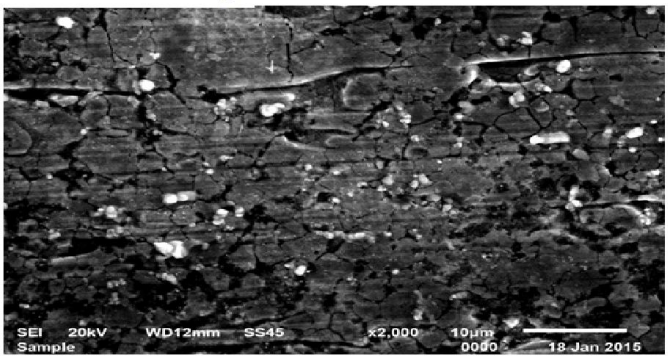

Figure 2. SEM of Bi- Pb- Sn- In based alloys

Table 2. Melting temperature and other thermal properties of $Bi_{50-x}Pb_{15}Sn_{22}Cd_3In_{10}(TiO_2)_x$ and Bi-Sn-Pb-Zn-In-Ag alloys

Alloys	Melting point ºC	C_P J/g. ºC	ΔS J/g. ºC	ρx 10^{-8} Ω. m	K $W.m^{-1}.K^{-1}$
$Bi_{49.5}Pb_{15}Sn_{22}Cd_3In_{10}(TiO_2)_{0.5}$	68.84	0.65	1.419	243.22	0.655
$Bi_{49}Pb_{15}Sn_{22}Cd_3In_{10}(TiO_2)_1$	91.37	0.408	0.119	228.31	0.696
$Bi_{48.5}Pb_{15}Sn_{22}Cd_3In_{10}(TiO_2)_{1..5}$	109.63	0.951	0.162	309.06	0.522

Alloys	Melting point ºC	C_P J/g. ºC	ΔS J/g. ºC	ρx 10^{-8}Ω. m	K $W.m^{-1}.K^{-1}$
$Bi_{25}Sn_{62.5}Pb_3Zn_3In_4Ag_{2.5}$	174.1	0.349	0.051	120.22	1.295
$Bi_{45.5}Sn_{42}Pb_3Zn_3In_4Ag_{2.5}$	123.16	0.966	0.238	176.34	0.893

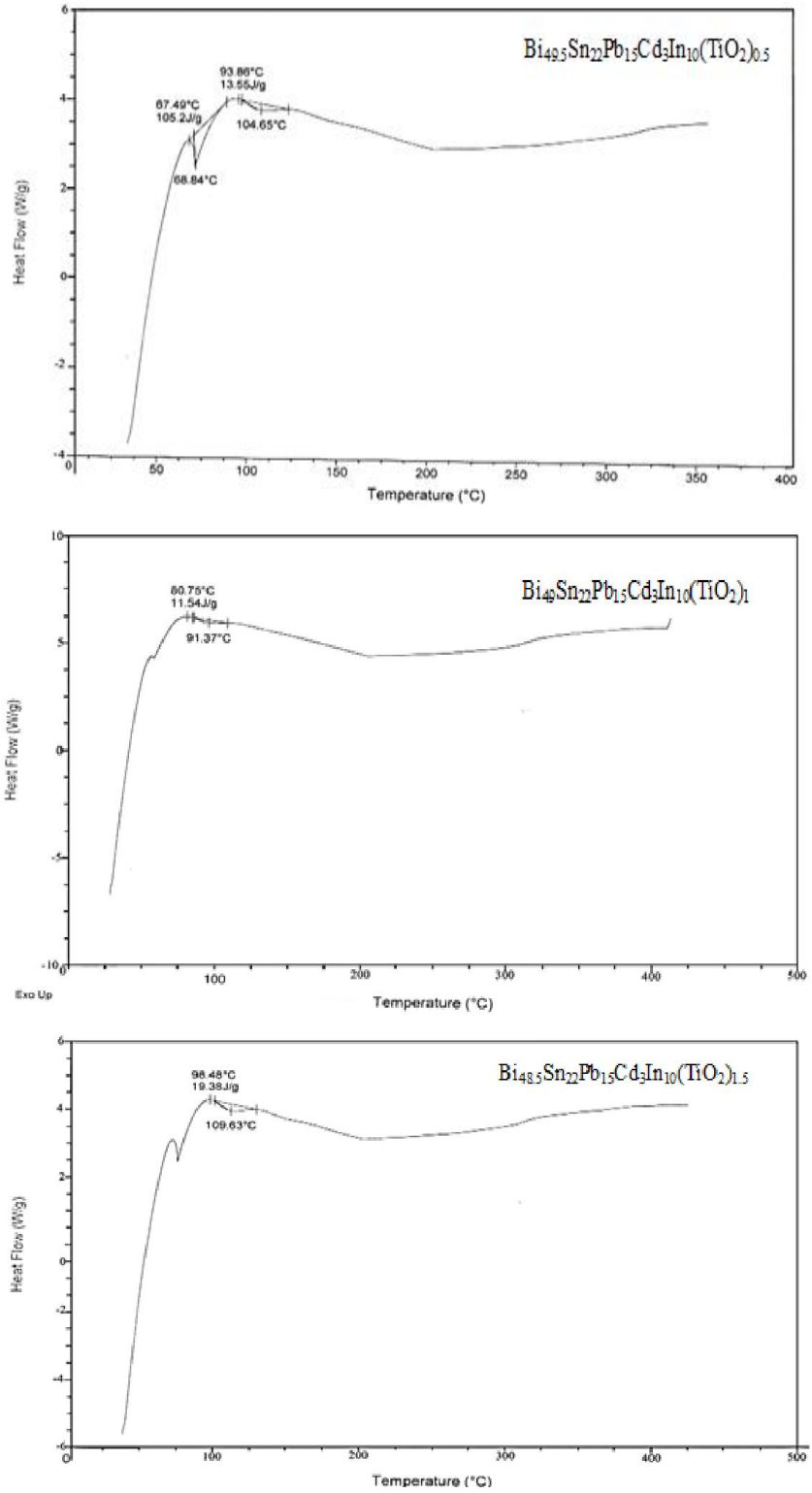

Figure 3a. DSC of $Bi_{50-x}Pb_{15}Sn_{22}Cd_3In_{10}(TiO_2)_x$ alloys

Table 3. elastic moduli, internal friction and thermal diffusivity of $Bi_{50-x}Pb_{15}Sn_{22}Cd_3In_{10}(TiO_2)_x$and Bi-Sn-Pb-Zn-In-Ag alloys

Alloys	E GPa	μGPa	B GPa	Q^{-1}	D_{th} x10^{-8} m^2\sec
$Bi_{49.5}Pb_{15}Sn_{22}Cd_3In_{10}(TiO_2)_{0.5}$	32.03	11.85	36.05	0.073	24.79
$Bi_{49}Pb_{15}Sn_{22}Cd_3In_{10}(TiO_2)_1$	36.16	13.38	40.61	0.055	42.82
$Bi_{48.5}Pb_{15}Sn_{22}Cd_3In_{10}(TiO_2)_{1..5}$	23.77	8.796	26.64	0.056	58.59

Alloys	E GPa	μGPa	B GPa	Q^{-1}	D_{th}x10^{-8} m^2\sec
$Bi_{25}Sn_{62.5}Pb_3Zn_3In_4Ag_{2.5}$	30.6	11.39	32.5	0.078	58.38
$Bi_{45.5}Sn_{42}Pb_3Zn_3In_4Ag_{2.5}$	31.34	11.72	32.05	0.073	21.59

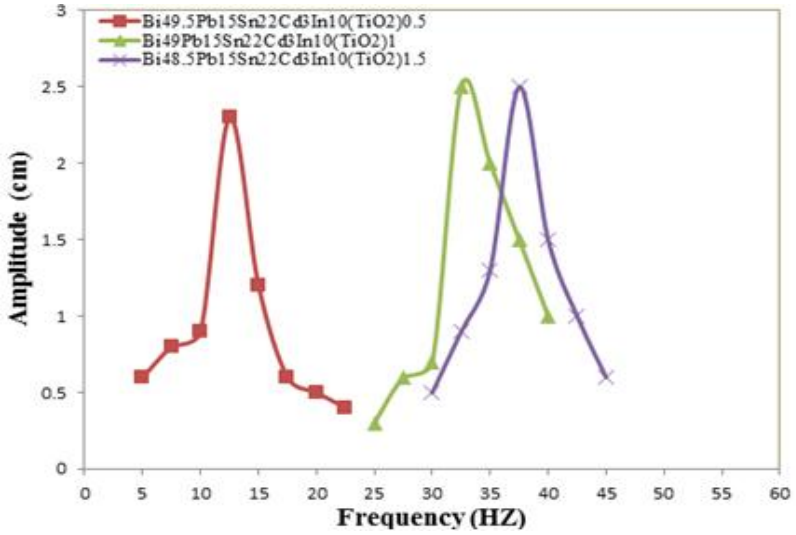

Figure 4a. Resonance curves of $Bi_{50-x}Pb_{15}Sn_{22}Cd_3In_{10}(TiO_2)_x$ alloys

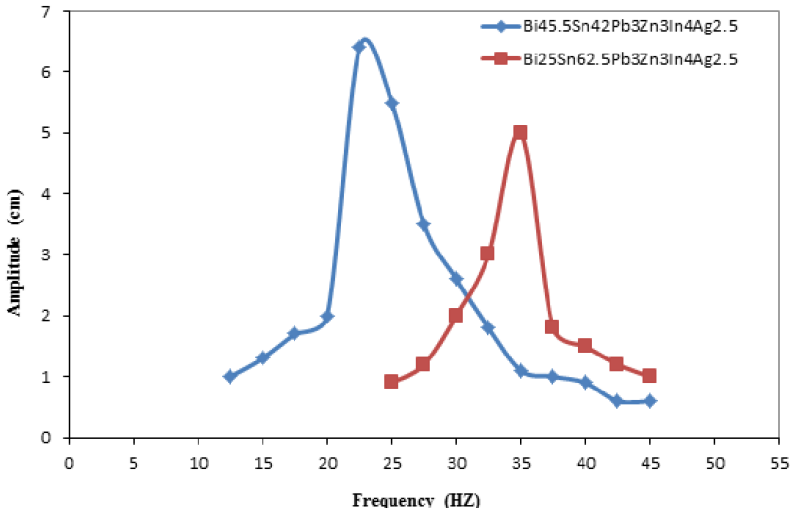

Figure 4b. Resonance curves of Bi-Sn-Pb-Zn-In-Ag alloys

Table 4. Vickers hardness and minimum shear stress of $Bi_{50-x}Pb_{15}Sn_{22}Cd_3In_{10}(TiO_2)_x$ and Bi-Sn-Pb-Zn-In-Ag alloys

Alloys	H_V Kg/mm^2	μ_n Kg/mm^2
$Bi_{49.5}Pb_{15}Sn_{22}Cd_3In_{10}(TiO_2)_{0.5}$	14.5±0.77	4.79
$Bi_{49}Pb_{15}Sn_{22}Cd_3In_{10}(TiO_2)_1$	19.05±0.63	6.27
$Bi_{48.5}Pb_{15}Sn_{22}Cd_3In_{10}(TiO_2)_{1.5}$	16.6±0.92	5.48

Alloys	H_v kg\mm^2	μ_n kg\mm^2
$Bi_{25}Sn_{62.5}Pb_3Zn_3In_4Ag_{2.5}$	19.25±0.92	6.35
$Bi_{45.5}Sn_{42}Pb_3Zn_3In_4Ag_{2.5}$	14.17±3.2	4.68

The results show variations on melting temperature, specific heat, enthalpy and thermal conductivity values of used alloys which dependent on its compositions.

Mechanical properties

The elastic properties of metallic materials are considerable significance to both science and technology. Their measurements yields information concerning the forces that are operative between the atoms comprising a melt-alloy, information that is fundamentally important in interpreting and understanding the nature of bonding in the solid state. Internal friction measurements have been quick fruitful for learning about the behavior of metallic materials. Also it can be used to determine thermal diffusivity. Elastic modului of $Bi_{50-x}Pb_{15}Sn_{22}Cd_3In_{10}(TiO_2)_x$, $Bi_{45.5}Sn_{42}Pb_3Zn_3In_4Ag_{2.5}$ and $Bi_{25}Sn_{62.5}Pb_3Zn_3In_4Ag_{2.5}$alloys are listed in Table 3. A significant change in elastic modulus values of $Bi_{50-x}Pb_{15}Sn_{22}Cd_3In_{10}(TiO_2)_x$ alloys with changing Tio_2 ratio.

But little variation caused in elastic modulus of Bi-Sn-Pb-Zn-In-Ag with changing Bi and Sn contents. The $Bi_{49}Pb_{15}Sn_{22}Cd_3In_{10}$ $(TiO_2)_1$ alloy has highest elastic modulus. The resonance curves of $Bi_{50-x}Pb_{15}Sn_{22}Cd_3In_{10}$ $(TiO_2)_x$, $Bi_{45.5}Sn_{42}Pb_3Zn_3In_4Ag_{2.5}$ and $Bi_{25}Sn_{62.5}Pb_3Zn_3In_4Ag_{2.5}$ alloys are shown in Figure 4 (a and b). Calculated internal friction and thermal diffusivity $Bi_{50-x}Pb_{15}Sn_{22}Cd_3In_{10}(TiO_2)_x$, $Bi_{45.5}Sn_{42}Pb_3Zn_3In_4Ag_{2.5}$ and $Bi_{25}Sn_{62.5}Pb_3Zn_3In_4Ag_{2.5}$ alloys are listed in Table 3 (a and b).

Internal friction values of $Bi_{50-x}Pb_{15}Sn_{22}Cd_3In_{10}$ $(TiO_2)_x$, $Bi_{45.5}Sn_{42}Pb_3Zn_3In_4Ag_{2.5}$ and Bi_{25} $Sn_{62.5}$ Pb_3 Zn_3 In_4 $Ag_{2.5}$ alloys varied. These variation dependent on alloys composition The $Bi_{49}Pb_{15}Sn_{22}Cd_3In_{10}$ $(TiO_2)_1$ alloy has low internal friction value. Hardness refers to various properties of matter in the solid phase that gives it high resistance to various kinds of shape change when force is applied. Hard matter is contrasted with soft matter. Macroscopic hardness is generally characterized by strong intermolecular bonds. Vickers hardness and calculated minimum shear stress values of Bi_{50-x} $Pb_{15}Sn_{22}Cd_3In_{10}(TiO_2)_x$, $Bi_{45.5}Sn_{42}Pb_3Zn_3In_4Ag_{2.5}$and $Bi_{25}Sn_{62.5}$ $Pb_3Zn_3In_4Ag_{2.5}$ alloys are listed in Table 4. The results show that, $Bi_{49}Pb_{15}Sn_{22}Cd_3In_{10}$ $(TiO_2)_1$ and $Bi_{25}Sn_{62.5}Pb_3Zn_3In_4Ag_{2.5}$ alloys have highest hardness value.

Conclusions

- All measured physical properties (thermal parameters, electrical resistivity, elastic moduli, internal friction and hardness) for used alloys effected by changing alloys compositions.
- The $Bi_{49}Pb_{15}Sn_{22}Cd_3In_{10}$ $(TiO_2)_1$has high strengthens such as elastic modulus and Vickers hardness but it has lower internal friction.
- The $Bi_{25}Sn_{62.5}Pb_3Zn_3In_4Ag_{2.5}$alloy hashigh values of hardness, internal friction and thermal diffusivity.

Recommendation

New prepared $Bi_{50-x}Pb_{15}Sn_{22}Cd_3In_{10}$ $(TiO_2)_x$ and Bi-Sn-Pb-Zn-In-Ag alloys have best properties for fuse electric and nuclear applications.

REFERENCES

Blackwell, C.R. and K. D. 1990. Amundson, Medical Dosimetry15 127-129.

Davis, J.B. and Reiner, B. 1995. Radiotherapy and Oncology 34 219-227.

El-Bediwi, A.B. 2002. A.M.S.E. 75:3 1–12 .

El-Bediwi, A.B. and. El-Bahay, M.M 2004. Radiation Effect and Defects in Solids 159 133–140.

El-Bediwi, A.B. El-Bahay, M.M. and Kamal, M. Radiation Effect and Defects in Solids 159 (2004) 491–496.

El-Bediwi, A.B. Said Gouda, E. and Kamal, M. 2004. A.M.S.E 65:1Modeling C.

Glazer, J. 1994. *Journal of Electronic materials,* 23: 8.

Kamal, M. Karman, M.B. and El-Bediwi, A.B. 1997. *U. Scientist Phyl. Sci.,* 9:2.164–171.

Kamal, M. and El-Bediwi, A.B. 2000. *J. Mater. Sci. Mater. Electr*., 11519–523.

Kamal, M. and El-Bediwi, A.B. 2004. Radiation Effect and Defects in Solids159. 651.

Kamal, M. El-Bediwi, A.B. and El-Ashram, T. 2004. *J. Mater. Sci. Mater. Electr***.**, 15 211–217.

Kamal, M. El-Tonsy, M., El-Bediwi, A.B. Kashita, E. 2004. *Phys. Stat. Sol.,* (a) 201**:**9 2029–2034.

Kamal, M., El-Bediwi, A.B. and Karman, M.B. 1998. *J. Mater. Sci. Mater. Electr.,* 9 425–428.

Kamal, M., Mazen, S., El-Bediwi, A.B. Kashita, E. 2006. Radiation Effect and Defects in Solids 161143-148

Kamal, M., Meikhail, M.S. and El- Bediwi, A.B. E. Said Gouda, Radiation Effect and Defects in Solids 160(2005) 37.

Marrs, J.E. Hounsell, A.R and Wilkinson, J.M. 1993. *The British journal of Radiology,* 66 140-144

McCormack, M.T., Degani, Y., Chen, H.S. and Gesick, W.R. 1996. *journal Jo.M.,* 48: 5 54-56.

Nuttall, K. 1971. *J. Inst. Met.* 99 266.

Powers, W.E., Kinzie, J.J., Demidecki, A.J. Bradfield, J. S. and Feidman, A. 1973. *Radiology,* 108 407-411.

Schreiber, E. Anderson, O. L. and Soga, N. 1973. Elastic Constants and Their Measurements (McGraw-Hill, New York, 82–125.

Timoshenko, S. and Goddier, J. N. Theory of Elasticity, 2nd ed. (McGraw-Hill, New York, 277

****